Cancer Management and Research

Dovepress

open access to scientific and medical research

Open Access Full Text Article

ORIGINAL RESEARCH

Ultrasound-Mediated Co-Delivery of miR-34a and sPD-1 Complexed with Microbubbles for Synergistic Cancer Therapy

This article was published in the following Dove Press journal:
Cancer Management and Research

Yu-e Qin*
Wen-fan Tang*
Yun Xu
Fu-rong Wan
Ai-hua Chen

Department of Gynecology and Obstetrics, The People's Hospital of China Three Gorges University/The First People's Hospital of Yichang, Yichang 443000, Hubei, People's Republic of China

*These authors contributed equally to this work

Background: miR-34a was downregulated and PD-L1 was upregulated in cervical cancer; however, the treatment of cervical cancer lacks precision and targeting. This study explored the ultrasound-mediated co-delivery of miR-34a and sPD-1 complexes with microbubbles for synergistic cancer therapy.

Methods: Cationic lipid microbubbles (CLMBs) were prepared by membrane hydration and mechanical oscillation. U14 subcutaneous xenograft mice were injected with CLMBs-loaded sPD-1 and miR-34a combined with ultrasound targeted destruction, and tumor volume and tumor weight of mice were measured. TUNEL apoptosis test and the mRNA expression of apoptosis-related gene Bcl-2 and Bax were analyzed by qRT-PCR. Antitumor immune-related cytokines IFN-γ were investigated by qRT-PCR, LDH Cytotoxicity Assay Kit were performed to test cytotoxic T lymphocytes (CTL).

Results: CLMBs were successfully prepared and the plasmid bound to its surface. The tumor volume and weight were specifically decreased by ultrasound-mediated co-delivery of miR-34a and sPD-1 complexes with microbubbles, apoptosis was induced and the apoptosis suppressor gene Bcl-2 was downregulated and proapoptotic gene Bax were upregulated. qRT-PCR analysis revealed that antitumor immunity-related IFN-γ was strongly upregulated in mice, which were treated with CLMBs-loaded sPD-1 and miR-34a combined with ultrasound targeted destruction, and the percentage of CTL was increased.

Conclusion: These findings from the study demonstrated that CLMBs could deliver miR-34a and sPD-1, combined with ultrasound targeted destruction, could suppress the tumor tissue growing, induce apoptosis and enhance antitumor immunity in U14 subcutaneous xenograft mice.

Keywords: miR-34a, sPD-1, microbubbles, ultrasound, cervical cancer, cancer therapy

Introduction

Cervical cancer is the fourth most common female malignancy worldwide and represents a major global health challenge, there were 569,847 new cases and 311,365 deaths reported in 2018.[1] Although the incidence of cervical cancer has been greatly reduced by the use of Human Papilloma Virus (HPV) vaccines and cervical cancer screening, the prevalence of cervical cancer has increased in developing countries.[2,3] For cervical cancer, traditional treatments include surgery, medication, and radiation therapy. Although a great deal of progress has been made, there are limitations with traditional treatments: surgery is invasive and risky, chemotherapy has many side effects, drugs have toxicity, and systemic adverse reactions have greatly reduced the quality of life of patients.[4] In recent years,

Correspondence: Ai-hua Chen
Department of Gynecology and Obstetrics, The People's Hospital of China Three Gorges University/The First People's Hospital of Yichang, No. 4, Hudi Street, Yichang City, Hubei Province, People's Republic of China
Tel +8613972602239
Fax +86717-6221636
Email m15071798480_2@163.com

submit your manuscript | www.dovepress.com
DovePress
http://doi.org/10.2147/CMAR.S238643

cervical cancer immunotherapy has made great progress, including DNA vaccine, recombinant vector vaccine, and using anti-PD-1 mAb nivolumab combination with ipilimumab to treat the relapsed or metastatic HPV-associated cancer, stage I/II clinical study for safety and efficacy of evaluation,[5] due to the current low number of cases and limited follow-up time, further research and results are announced.

Through the cancer immunoediting process, tumor cells have acquired a variety of methods to evade host immunity in the tumor microenvironment, known as cancer immune escape.[6] Programmed death-l (PD-1) is a costimulatory molecule on the surface of T cells, and is an important negative immune regulatory molecule belonging to the CD28/CTLA-4 family. PD-1 ligand of programmed death-1 (PD-L1), which is a ligand for the immunosuppressive receptor PD-1, is widely expressed in most tumor tissues. PD-L1 interacts with PD-1 on the surface of T cells, inhibits the activation of tumor antigen specific T cells, and induces immune tolerance of T cells to tumor cells. This might be one of the important mechanisms by which tumor cells evade immune surveillance.[7,8]

PD-L1 expression was found in 96% of cervical cancer,[9] while expression of PD-L1 in histologically normal cervical tissues was rarely found. Meng et al reported that 60.82% (59/97) of the patients exhibited PD-1 expression in the tumor stroma of cervical cancer.[10] These data suggest that both PD-L1 and PD-1 are widely expressed in cervical cancer tumor cells and stroma, providing potential therapeutic targets for PD-1/PD-L1 inhibitors.

The PD-1/PD-L1 pathway-mediated negative signal can effectively prevent the activation of T cells in tumors and lead to immunosuppression, which is one of the main ways for tumors to evade immune system attacks.[11] Several studies have shown that blocking this signaling pathway by using PD-1 inhibitor can maintain T cell function, and enhance autoimmune killing. Anti-PD-1 antibodies have achieved significant results in clinical trials for the treatment of melanoma, lung cancer and renal cell carcinoma.[12,13] Soluble PD-1 (sPD-1) can be formed by proteolytic cleavage of membrane-type molecules on cells, or directly by specific mRNA expression. Studies have confirmed that sPD-1 can promote the body's antitumor immunity by effectively blocking PD-L1.

MiRNA (microRNA) is a non-coding RNA fragment with 21–23 nucleotides in length. The role of miRNAs in immune regulation is mainly concentrated in neoplastic diseases, miRNAs involved in the control of the activity and the recruitment of the immunosuppressive MDSCs to the tumor microenvironment, miRNAs also can induce NK cells and restore their antitumor activity.[14] MiR-34a was downregulated in cervical cancer,[15] but there are few studies on the function of miR-34a for cervical cancer. Cortez et al reported that miR-34a targeted PD-L1 in non-small cell lung cancer,[16] this suggests that there maybe a close relationship between miR-34a and PD-1/PD-L1 pathway in cervical cancer.

Molecular targeted therapy for tumors has also been extensively studied, gene-based tumor targeted therapy has proven to be promising in many experimental and preclinical studies,[17] however, the inefficiency and safety issues of gene delivery limit the potential of this treatment. Ultrasound and microbubble transfer genes can protect genes from degradation, at the same time, cavitation and pore effects caused by ultrasonic rupture of microbubbles significantly improve gene transfection efficiency, and the safety of microbubbles is better than that of commonly used virus carriers.[18,19]

Microbubble-mediated DNA delivery as an effective targeted therapy was reported in 1996.[20] Over the years, ultrasound microbubble-mediated gene therapy research has never been interrupted, including tumors, thrombosis and cardiovascular disease.[21,22] As a cavitation nucleus, microbubbles can oscillate, shrink, swell or even rupture under ultrasonic radiation of a certain frequency. Cavitation and somatoporation enhance cell membrane permeability and promote gene release.[23–25] Studies have shown that ultrasound microbubble contrast agents can not only enhance ultrasound imaging, but also serve as a novel gene carrier for treatment to achieve integration of diagnosis and treatment.[26,27] Molecular targeted therapy has gradually been applied in the clinic, but the key point is to choose the right target.

In this study, we use cationic lipid microbubbles (CLMBs) loaded sPD-1 (sPD-1/CLMBs), CLMBs loaded miR-34a (miR-34a/CLMBs), combined with sPD-1 and miR-34a/CLMBs, then apply ultrasound targeted microbubble destruction to achieve local release of the gene. We found that CLMBs and ultrasound could deliver sPD-1 and miR-34a to inhibit tumor growth and increase antitumor activity in cervical cancer. It suggests that CLMBs could be used as an ideal carrier for gene-targeted therapy, and this may provides a new way for the clinical treatment of cervical cancer.

Materials and Methods

Preparation of Cationic Lipid Microbubbles (CLMBs)

The CLMBs were composed of a perfluoropropane gas core, which contain dipalmitoyl phosphatidylcholine (DPPC;

Avanti Polar Lipids, Alabaster, AL, USA), 1,2-distearoyl-sn-glycero-3-phosphoethanolamine-N-[maleimide (polyethylene glycol)-2000] (DSPE-PEG2000; Avanti Polar Lipids) and 3β-[N-(N',N'-dimethylaminoethane)-carbamoyl] cholesterol hydrochloride (DC-Chol; Avanti Polar Lipids), DC-Chol provided a positively charged surface for the cationic microbubbles.

The mixture was evaporated under reduced pressure at 40°C for 1 h in a rotary evaporator, and dried under vacuum for 3 h, then add the prepared glycerin and PBS, sonicate in the ultrasonic cleaner until the film fell off, bathed with 45°C water for 1 h, then the solution was placed in a sealed glass vial bottle and the upper space was filled with perfluoropropane gas (C3F8) to obtain gas-filled CLMBs by a self-made gas exchange device, the CLMBs solution was stored at 4°C. The gene loaded CLMBs were prepared by incubating CLMBs with a plasmid in a certain ratio. The concentration is calculated using a hemocytometer, and the particle size and zeta potential is measured by Zetasizer Nano ZSP (Malvern Instruments, Malvern, UK).

Construction of Plasmid DNA

The genomic sequence of miR-34a (NCBI Gene 723848) and sPD-1 (GenBank: X67914.1) were acquired from NCBI, PCR primers were designed by Primer 5.0, and the miR-34a precursor was obtained by PCR amplification. The plasmid pcDNA3.1 (+) and the purified PCR product were digested with EcoR I and Xho I respectively, miR-34a and sPD-1 were ligated to plasmid pcDNA3.1(+) respectively by ligating with T4 ligase, constructed miR-34a-pcDNA3.1(+), sPD-1-pcDNA3.1(+) plasmid were sent to gene company (Sangon Biotech, Shanghai, China) for sequencing.

Preparation of Plasmid-CLMBs Complex

The plasmid is negatively charged and can be combined with CLMBs by electrostatic interaction. In order to optimize the suitable plasmid concentration, 1 μg plasmid was combined with 2.5 μL, 5 μL, 10 μL, 15 μL CLMBs and incubated at room temperature for 30 min. CLMBs/DNA complex was used as a sample for gel electrophoresis to observe the DNA loading capacity of CLMBs, the uncombined plasmid with negative charge will protrude toward the positive electrode and leave a bright band on the gel, while the CLMBs/DNA complex have slower band since the negatively charged plasmid binds to the CLMBs. In order to observe the binding of plasmids and CLMBs under a confocal microscope, we used PI (50 μg/mL) staining plasmids for 15 min, then added CLMBs and incubated for 30 min, and observed the binding of plasmid to CLMBs by confocal microscopy (Nikon Corporation, Tokyo, Japan).

Cell Culture

U14 cell lines were purchased from the China Center for Type Culture Collection (CCTCC, Wuhan, China). U14 cells were grown in DMEM (Thermo Fisher Scientific, Waltham, MA, USA) supplemented with 10% FBS (Thermo Fisher Scientific), and 1% penicillin/streptomycin (Thermo Fisher Scientific) at 37°C, 5% CO^2.

Establishment of a Subcutaneous Xenograft Model of Mouse U14 Cervical Cancer

SPF female BALB/c mice 4–6 week old, 18–21 g, were purchased from the Animal Laboratory Center of China Three Gorges University (CTGU, Yichang, China). The animal study was approved by the medical ethics committee of China Three Gorges University, and followed the principles of National Institutes of Health for the care and use of laboratory animals,[28] with all efforts being made to minimize pain.

Prepared U14 cells were injected into the peritoneal cavity of two mice when the U14 cells were in good condition. After eight days, ascitic fluid was taken and the cell concentration was diluted to 1×10^7 cells/mL, 0.2 mL of the cell suspension was inoculated into the right anterior armpit of the mouse to form a tumor.

Forty mice successfully modeled were randomly divided into five groups, each group hadeight mice, and the mice were injected with 200 μL (2.310^8/mL) corresponding CLMBs from the tail vein. Group A, negative control, the mice were injected from the tail vein into mouse with 0.9% NaCl; Group B, the mice were injected with CLMBs; Group C, CLMBs/sPD-1-pcDNA3.1 plasmid complexes were injected (sPD-1); Group D, CLMBs/miR34a-pcDNA3.1 plasmid complexes were injected (miR34a); Group E, CLMBs combined with sPD-1-pcDNA3.1 plasmid and miR34a-pcDNA3.1 plasmid were injected into mice (Combined). The mice were injected every two days, and received a total of five injections and treatments.

After injection the low-frequency ultrasound irradiation (frequency 1 MHZ, power 1.5 W/cm^2, duty cycle 50%, irradiation time 90 s) were taken in the tumor immediately, so the genes were locally released in tumors. After

inoculation, animals were observed every day, tumor size was determined by measuring two diameters perpendicular to each other with a caliper at days 5, 10, 15, and 20. Tumor volume was calculated according to the following equation: V (mm^3) = $width^2(mm^2)$×length (mm)/2. On day 20, animals were humanely sacrificed, tumor masses were rapidly removed and weighed.

TUNEL Assay

TdT-mediated dUTP nick end labeling (TUNEL) staining was carried out using the cell apoptosis detection kit (Hoffman-La Roche Ltd, Basel, Switzerland) according to the manufacturer's instructions. The tissues present obvious apoptotic cells were regarded as positive control, and the reagent 2 (deoxyribonucleic acid mixture) without terminal TdT instead of TUNEL reaction mixture was regarded as negative control. We used a confocal microscope to observed each tissue sections. Nuclei with clear red staining were regarded as positive.

qRT-PCR

In brief, the total RNA was extracted from collected samples with using TRIzol reagent (Thermo Fisher Scientific, Waltham, MA, USA). MiraMasTM Kit (Bioo Scientific, Austin, TX, USA) was applied to perform the reverse-transcription reactions. RT-PCR analyses for genes were done with using SYBR green (Takara Bio Inc., Shiga, Japan) on applied biosystems 7500 real-time PCR system (primers showed in Table 1). Moreover, using GAPDH as an internal reference, the relative expressions of mRNAs were analyzed with the comparative cycle threshold (CT) method-fold change (2−ΔΔCT).

Cytotoxic T Lymphocytes (CTL)

The spleen of mice were dissociated in medium. Red blood cells were lysed with red blood cell lysis buffer. Finally, cells were adjusted to 1×10^6/mL and co-cultured with U14 cell lysis (100 μg/well) in the 24-well plate for three to five days, then the cells were collected and co-cultured with U14 cells in the 96-well plate at the ratio of 50:1 for 6 h. Next, the liquid supernatant was collected and detected with the LDH Cytotoxicity Assay Kit (Beyotime, Shanghai, China) according to LDH kit instruction.

Table 1 Lists of primers for PCR reaction

Genes	Primer	Sequences of Primer (5′ to 3′)
GAPDH	Forward Reverse	GGTGGTCTCCTGTGACTTCAA CCACCCTGTTGCTGTAGCC
Bcl-2	Forward Reverse	CGTCAACAGGGAGATGTCACC CAGCCAGGAGAAATCAAACAGAG
Bax	Forward Reverse	TGGTTGCCCTCTTCTACTTTGC CAGACAAGCAGCCGCTCAC
INF-γ	Forward Reverse	CCATCGGCTGACCTAGAGAA GATGCAGTGTGTAGCGTTCA

Statistical Analysis

The data were analyzed by SPSS18.0 software. The measurement data were expressed by x±s. The comparison between groups was performed by one-way analysis of variance (ANOVA). The comparison between the two groups was performed by LSD (t-test). $P<0.05$ was considered statistically significant, and $P<0.01$was considered significant statistical difference.

Results

Characterization of Cationic Microbubbles (CLMBs)

CLMBs were successfully prepared by membrane hydration and mechanical oscillation. The concentration of the CLMBs was determined by hemocytometer, the size (Figure 1F) and the surface zeta potential of CLMBs were determined via Zetasizer Nano ZSP detector, the CLMBs have a mean diameter of 700.7±193.8 nm, consistent with the clinical ultrasound contrast agent particle size requirements.[29] As shown in Table 2, the concentration of the CLMBs was $(2.3\pm0.5)\times10^8$/mL. CLMBs have a mean surface zeta potential (24.7±6.8 mV), so the plasmid can bind to the CLMBs by electrostatic adsorption, as demonstrated in Figure 1B, we used PI staining plasmids, and then added CLMBs and incubated for 30 min, the red fluorescence represents that the plasmid combined to CLMBs, there was no red fluorescence in Figure 1A which just has CLMBs, in order to select the optimal concentration of plasmid bound to CLMBs, the agarose gel electrophoresis was used to observe the DNA band, the result showed that 1 μg plasmid can electrostatically adsorb 15 μL CLMBs (Figure 1E), suggesting that each 1×10^8 microbubbles can bind 28 μg plasmid. CLMBs were smooth, spherical, stable shape and uniform particle size under laser confocal microscope (Figure 1C), the Figure 1D was shown the CLMBs combine with plasmids under laser confocal microscope, there has not been much change in size and shape.

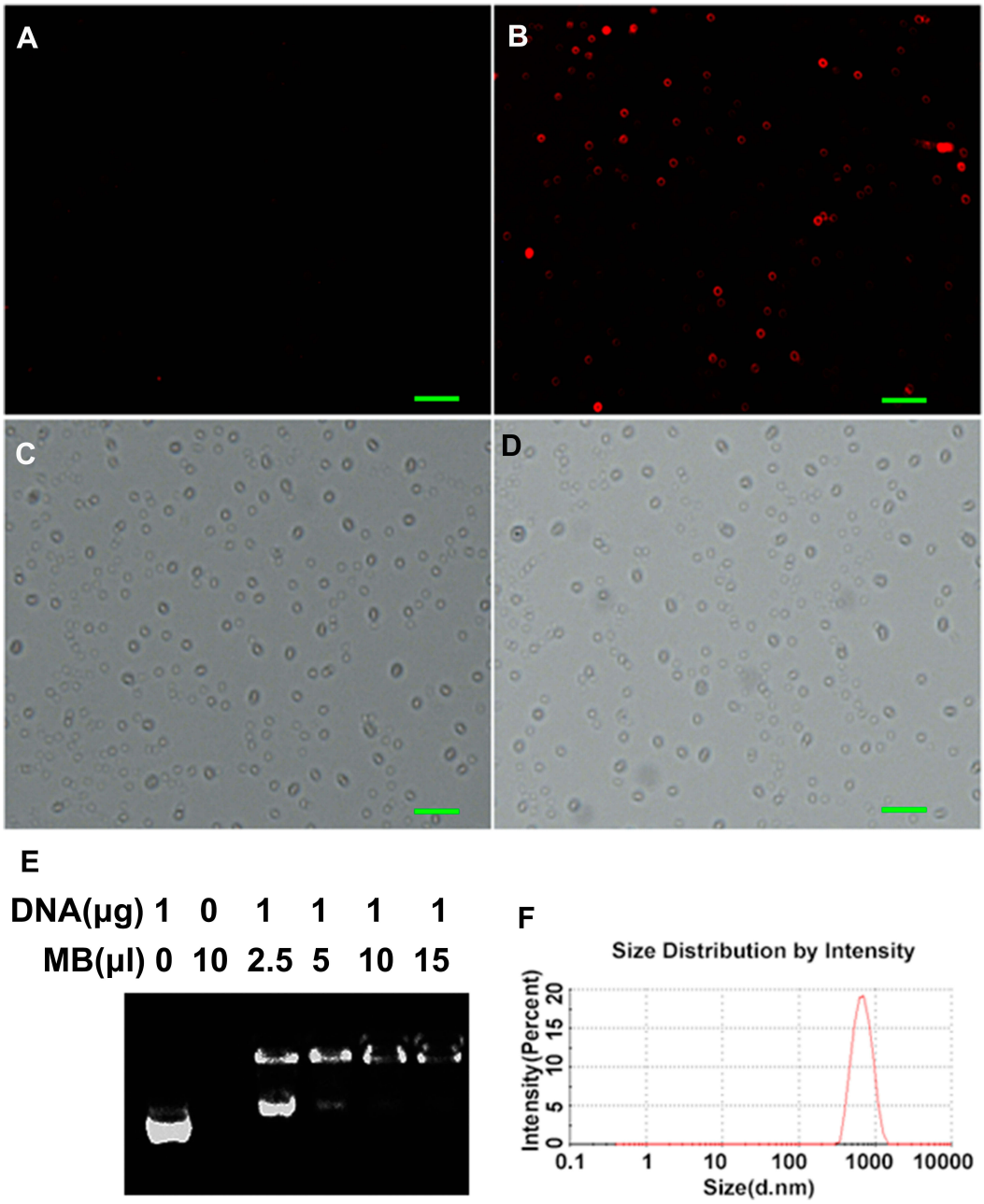

Figure 1 Characterization of cationic microbubbles (**A**–**F**). The scan bar: 5μm.

Ultrasound-mediated Co-delivery of miR-34a and sPD-1 Complexed with Microbubbles Suppresses the Tumor Tissue Growing of U14 Subcutaneous Xenograft Mice

In 2006, a clinical study of the use of PD-1 pathway inhibitors in the treatment of drug-resistant solid tumors was initiated in the United States. Brahmer et al reported that the first phase clinical trial of anti-PD-1 antibody MDX-1106 was performed in 39 patients with metastatic cancer.[30] He constructed a soluble PD-1 plasmid (sPD-1), confirming that cytokines and costimulatory lymphocytes can be regulated by sPD-1 blockade, and that PD-1/B7-H1 may be blocked by the sPD-1 pathway.[31] Whether using PD-1 antibody or sPD-1 plasmid to treat tumors, the principle is to block PD-1/PD-L signaling pathway, reversed inhibition of T cell function, and enhance

Table 2 The Characteristics of Cationic Lipid Microbubbles (CLMBs)

	Concentration (10^8/mL)	The Average Diameter (nm)	Zeta Potential (mV)
CLMBs	2.30.5	700.7193.8	24.76.8

immune killing. In this study, we constructed sPD-1 plasmid bind to the CLMBs, and combined with ultrasound to explore whether CLMBs/sPD-1 combined with ultrasound can suppress the tumor tissue growing of U14 subcutaneous xenograft mice.

In our previous research, miR-34a was downregulated in cervical cancer, in this study we constructed miR-34a plasmid to bind to the CLMBs, and use ultrasound targeted microbubble destruction, to investigate whether miR-34a can inhibit the growth of tumor tissue in U14 subcutaneous xenograft mice.

In order to study the tumor suppression of miR-34a, sPD-1 and the combination of the two, we designed five groups of experiments, group 1 and group 2 were control groups (0.9% NaCl+US) and CLMBs group (CLMBs+US) respectively, the tumor volume of mice in the control group grew rapidly, and some mice had dyskinesia in the forelimbs, while group 3 (CLMBs/sPD-1+US), group 4 (CLMBs/miR-34a+US) and group 5 (CLMBs/sPD-1+CLMBs/miR-34a+US) had different degrees of reduction on tumor volume and tumor mass, especially in group 5 (Figure 2A and B and Table 3).

These results indicate that ultrasound-mediated co-delivery of miR-34a and sPD-1 complexes with microbubbles can effectively inhibit tumor growth in U14 subcutaneous xenograft mice.

Ultrasound-mediated Co-Delivery of miR-34a and sPD-1 Complexed with Microbubbles (sPD1+miR-34a+US) can Induce Apoptosis in Tumor Tissues

We confirmed that miR-34a and sPD-1 inhibits tumor growth through CLMBs and ultrasound targeted destruction, then we used the TUNEL apoptosis test to study the effect of ultrasound-mediated co-delivery of miR-34a and sPD-1 complexed with microbubbles in tumor tissue of mice, the result was presented in Figure 3A, in group 4 (miR-34a) and group 5(sPD-1+miR-34a) apoptotic cells increased significantly, red-stained nuclei indicate that the cells are in an apoptotic state, there were a large number of apoptotic cells appeared in the

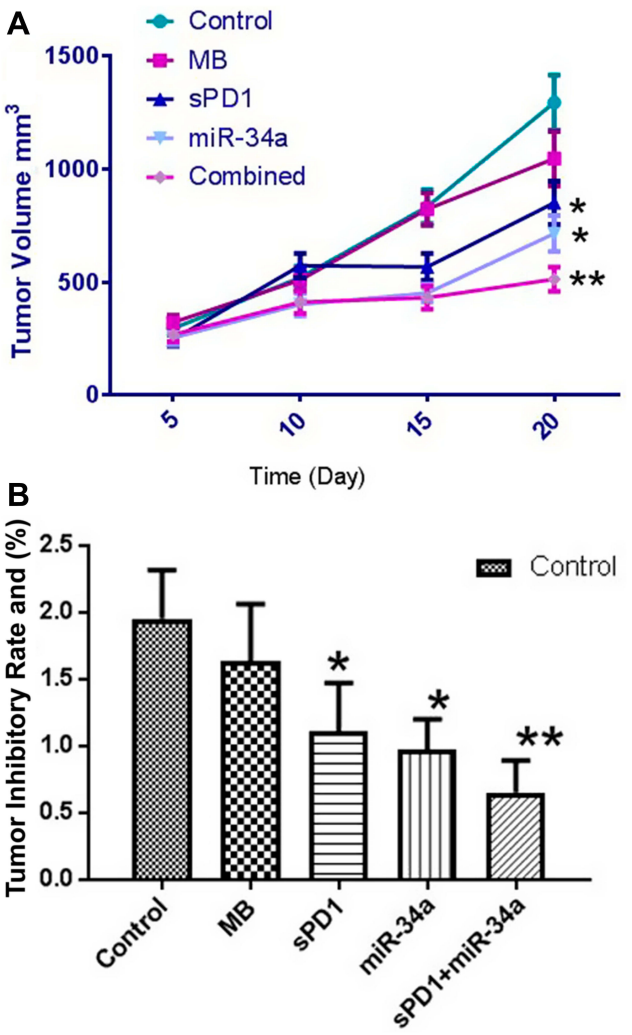

Figure 2 Tumor volume (**A**) and tumor weight (**B**) in each group. *$P \leq 0.05$. **$P \leq 0.01$.

tumor tissues of group 4 and group 5. These results indicated that miR-34a can induce apoptosis, therefore we continue to detect the mRNA expression of apoptosis-related gene Bcl-2 and Bax. The Bcl-2 is a proto-oncogene that inhibits apoptosis by altering the

Table 3 Tumor Volume and Tumor Weight in each Group

Group	Tumor Volume (mm^3)	Tumor Weight (g)
Control	1294.77±121.84	1.95±0.36
MB	1046.64±120.83	1.63±0.43
sPD1	850.57±96.32*	1.11±0.36*
miR-34a	714.62±80.32*	0.97±0.23*
Combined	512.35±54.04**	0.65±0.24**

Notes: *$P \leq 0.05$. **$P \leq 0.01$.

Abbreviations: Control, 0.9% NaCl+ultrasound; MB, cationic lipid microbubbles +ultrasound; sPD1, cationic lipid microbubbles/sPD-1+ultrasound; miR-34a, cationic lipid microbubbles/miR-34a+ultrasound; Combined, cationic lipid microbubbles/sPD-1+cationic lipid microbubbles/miR-34a+ultrasound.

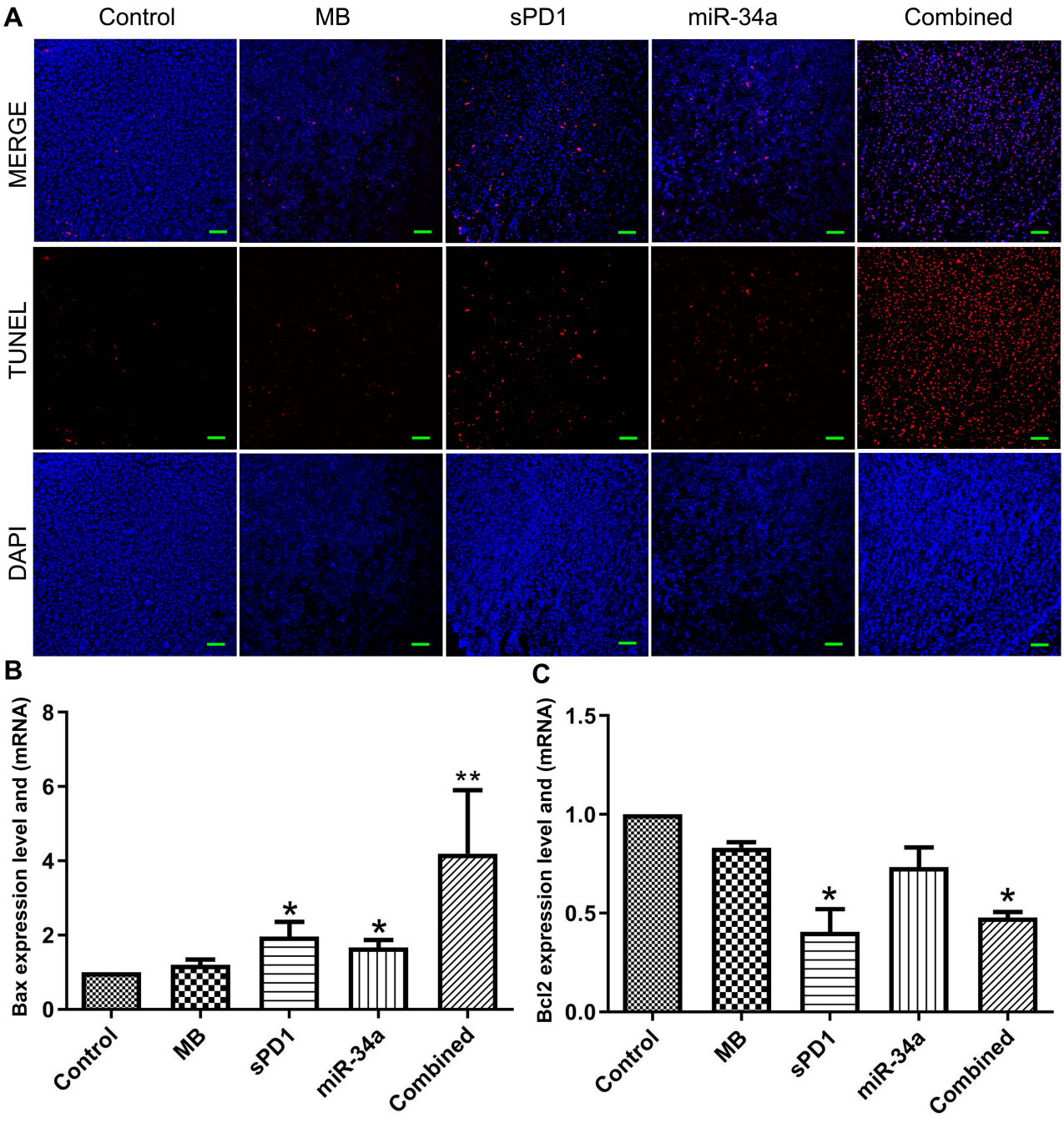

Figure 3 Apoptosis and relative gene expression in tumor tissues (**A**–**C**). *$P \leq 0.05$. **$P \leq 0.01$.

permeability of mitochondrial membranes to apoptotic protein precursors. Bax is a water-soluble protein homologous to Bcl-2 and is an apoptosis-promoting gene in the Bcl-2 gene family. As shown in Figure 3B, Bax was downregulated in the control group and upregulated in sPD-1 group and miR-34a group,especially in co-delivery of miR-34a and sPD-1 complexed group. The expression of Bcl-2 were shown in Figure 3C, the sPD-1 group and the combined group were downregulated.

Ultrasound-mediated Co-Delivery of miR-34a and sPD-1 Complexed with Microbubbles (sPD1+miR-34a+US) Enhance Anti-Tumor Immunity

Interferon-gamma (INF-γ) is produced by immune cells such as activated macrophages, T cells, natural killer cells, which can affect the body's immune regulation function, and enhance the body's antitumor immunity. So we

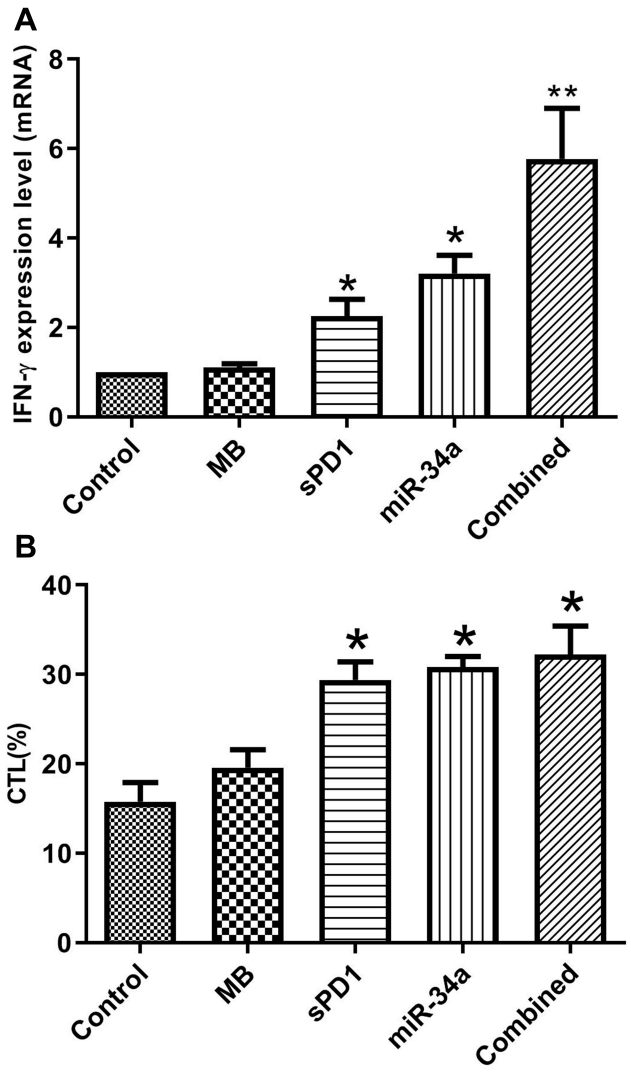

Figure 4 CLMBs/sPD-1+CLMBs/miR-34a+US enhance antitumor immunity (**A, B**). *$P \leq 0.05$. **$P \leq 0.01$.

used qRT-PCR to detect the expression of IFN-γ in the tumor tissues. Figure 4A demonstrates that sPD-1+miR-34a+US can effectively promote the expression of INF-γ, and the gene combination (sPD-1+miR-34a+US) is more effective than a single gene (sPD-1 or miR-34a).

In order to explore the effect of sPD1+miR-34a+US on the specific T lymphocytes, lactate dehydrogenase cytotoxicity assay kit (LDH cytotoxicity assay kit) was used to detect cytotoxic T lymphocytes (CTL). Cytotoxicity or mortality (%) = (treatment sample absorbance – sample control well absorbance)/(absorbance of cell maximum enzyme activity – sample control well absorbance) ×100. The results shown in Figure 4B and Table 4 that the cytotoxicity was enhanced, especially in group 5 (sPD-1 +miR-34a+US).

Table 4 The Percentage of CTL in each Group

Group	CTL (%)
Control	15.77
MB	19.57
sPD1	29.37*
miR-34a	30.85*
Combined	32.2*

Note: *$P \leq 0.05$.
Abbreviations: Control, 0.9% NaCl+ultrasound; MB, cationic lipid microbubbles +ultrasound; sPD1, cationic lipid microbubbles/sPD-1+ultrasound; miR-34a, cationic lipid microbubbles/miR-34a+ultrasound; Combined, cationic lipid microbubbles/ sPD-1+cationic lipid microbubbles/miR-34a+ultrasound.

Discussion

In the past several years, targeted cancer therapy has drawn increased attention to the studies on targeted gene therapy. Targeted therapy is the treatment of a well-defined carcinogenic site at the cellular level. It is most important to select specific targets, stable vectors and effective therapeutic drugs or genes.[32–34] Ultrasound-targeted microbubble disruption (UTMD) technology is a promising novel approach for targeted gene and drug delivery. In particular, it has been shown that these techniques can achieve better gene delivery efficiency than viral vectors by increasing cell membrane permeability.[35]

The CLMBs used in this study could be efficiently loaded with DNA-lipoplexes. The particle size of the microbubbles prepared by membrane hydration in this study is nanometer-scale and stable, and they have a mean surface zeta potential (24.7±6.8 mV), which is comparable to the size of commercially available microbubbles, DNA-loading did not significantly alter the mean CLMBs diameter. Fan et al used PI staining plasmids to verify their binding to microbubbles, they observed red fluorescence around the microbubbles under a laser confocal microscope,[34] we used the same method to verify that plasmid can binds to CLMBs effectively. Studies have shown that the capacity of CLMBs loading plasmid can reach saturation,[25] so we applied gel electrophoretic test for checking plasmid affinity of CLMBs, our results shown that 1 μg plasmid can be saturated with 15 μL CLMBs, and this is consistent with the literature.

In our study we use CLMBs loaded sPD-1 (sPD-1/ CLMBs) then injected intravenously into U14 subcutaneous xenograft mice. Appropriate ultrasound were conducted in the local mass of mice. In the case of our mice we could observe that the volume of tumor tissue is smaller than the control group, interestingly, the tumor volume of the empty microbubble group is also smaller

than the control group, this may be associated with microbubble-enhanced ultrasound cavitation effect, which can effectively damage the microvessels of the tumor tissue and cause perfusion defects in the tumor area.

Microbubbles loaded sPD-1 (sPD-1/CLMBs) can effectively bind to the PD-L1, and the PD-1/PD-L1 signaling pathway on lymphocytes is inhibited, which can effectively improve the T cell function and enhance antitumor immunity.

Blocking the PD-1/PD-L1 negative signaling pathway can significantly affect the secretion of related cytokines. sPD-1 has been reported to reduce IFN-γ-mediated immunosuppression.[36] In our study we found that the level of IFN-γ was increased in miR-34a/CLMBs group and sPD-1/CLMBs group, especially in simultaneous injection of miR-34a/CLMBs and sPD-1/CLMBs groups.

In addition to sPD-1, we also use microbubbles loaded miR-34a, several studies have indicated that 30–50% of human gene expressions are probably controlled by miRNAs, including cell proliferation, differentiation, apoptosis, immune regulation. It is conceivable that miRNAs will play a critical role in the occurrence of cervical cancers and can potentially serve as biomarkers and targets for anticancer therapy. MiR-34a has been reported to be a key regulator of tumor suppression and downregulated in several cancers, in our previous studies, we demonstrated that miR-34a was a novel biomarker upexpression in cervical cancer. In this study, we found that miR-34a/CLMBs combined with ultrasound can suppresses the tumor tissue growing of U14 subcutaneous xenograft mice, and this inhibition was more obvious when mixing the miR-34a/CLMBs and sPD-1/CLMBs.

MiR-34a is targeted several molecules that are involved in proliferation, apoptosis, invasion, metastasis and epithelial mesenchymal transition of cancer cells.[37–39] In our research, we found apoptosis were observed in both miR-34a/CLMBs group, and the miR-34a/CLMBs and sPD-1/CLMBs mixed group, it might be through Bcl-2 which is targeted by miR-34a. B-cell lymphoma-2 (Bcl-2) is a proto-oncogene that inhibits apoptosis by modulating the permeability of mitochondrial membranes to apoptotic protein precursors. Bcl-2 related X (Bax) is a homologous to Bcl-2 and an apoptosis-promoting gene in the Bcl-2 gene family.[40–42] Overexpression of Bax can antagonize the protective effect of Bcl-2 and lead to cell death. Our results shown that Bcl-2 were down expression in miR-34a/CLMBs group and miR-34a/CLMBs and sPD-1/CLMBs mixed group. To further verify whether miR-34a/CLMBs combined with ultrasound can promotes tumor cell apoptosis, we performed a TUNEL experiment, which showed that a large number of apoptotic cells appeared in the tumor tissues of the miR-34a/CLMBs group and miR-34a/CLMBs and sPD-1/CLMBs mixed groups, which demonstrated that microbubbles loaded the miR-34a combined with ultrasound can effectively mediate gene transfection.

In our study, we found that CLMBs loaded sPD-1 inhibits the growth of cervical cancer, and also the miR-34a, more importantly, when we injected the mix of miR-34a/CLMBs and sPD-1/CLMBs, then used ultrasound-targeted microbubble destruction, we observed additive effect, this maybe associated with miR-34a target PD-L1 in cervical cancer, and this targeted relationship has been reported in several cancers, such as glioma cells, B-cell lymphomas, non-small cell lung cancer.[43,44]

In conclusion, CLMBs can be an effective carrier to delivery the DNA to the cancer or maybe other target, as shown in this study, ultrasound-targeted microbubble destruction enhance gene delivery, it is suggested that the clinical applications of MBs for cancer treatment purposes are clearly promising because this delivery is safe and efficient, and this provides new ideas and guidelines for the clinical treatment of cancer.

Conclusion

Based on previous studies which have demonstrated that microbubble-mediated DNA delivery is an effective targeted therapy, we found that CLMBs-mediated miR-34a and sPD-1 delivery suppressed the growth of tumor tissue,induced apoptosis and enhanced antitumor immunity in U14 subcutaneous xenograft mice. It is suggested that CLMBs-mediated miR-34a and sPD-1 delivery is an effective targeted therapy in cervical cancer U14 subcutaneous xenograft mice.

Ethical

The animal study was approved by the medical ethics committee of China Three Gorges University, and followed the principles of the National Institutes of Health for the care and use of laboratory animals, with all efforts being made to minimize pain. The U14 cell were purchased from the China Center for Type Culture Collection (CCTCC, Wuhan, China) and approved by the medical ethics committee of China Three Gorges University.

Acknowledgments

This research was supported by Open FoundationProject of Hubei Key Laboratory of Tumor Microenvironment

and Immunotherapy (China Three Gorges University, 2016KZL06).

Disclosure

The authors declare that there is no conflict of interest in this work.

References

1. Bray F, Ferlay J, Soerjomataram I, et al. Global cancer statistics 2018: GLOBOCAN estimates of incidence and mortality worldwide for 36 cancers in 185 countries. *CA Cancer J Clin*. 2018;68:394–424. doi:10.3322/caac.v68.6
2. Liu YC, Wu L, Tong RZ, et al. PD-1/PD-L1 inhibitors in cervical cancer. *Front Pharmacol*. 2019;10:65. doi:10.3389/fphar.2019.00065
3. Goodman A. HPV testing as a screen for cervical cancer. *BMJ*. 2015;350:h2372. doi:10.1136/bmj.h2372
4. Rotman J, Mom CH, Jordanova ES, et al. 'DURVIT': a phase-I trial of single low-dosedurvalumab (Medi4736) IntraTumourallyinjected in cervical cancer: safety, toxicity and effect on the primary tumour- and lymph node microenvironment. *BMC Cancer*. 2018;18:888. doi:10.1186/s12885-018-4764-0
5. Mayadev J, Zamarin D, Deng W, et al. Anti-PD-L1 (atezolizumab) as an immune primer and concurrently with extended-field chemoradiotherapy for node-positive locally advanced cervical cancer. *Int J Gynecol Cancer*. 2019;001012.
6. Gonzalez H, Hagerling C, Werb Z. Roles of the immune system in cancer: from tumor initiation to metastatic progression. *Genes Dev*. 2018;32:1267–1284. doi:10.1101/gad.314617.118
7. Chen ZF, Pang NN, Du R, et al. Elevated expression of programmed death-1 and programmed death ligand-1 negatively regulates immune response against cervical cancer cells. *Mediators Inflamm*. 2016;6891482.
8. Komiya T, Madan R. PD-L1 expression in small cell lung cancer. *Eur J Cancer*. 2015;51:1853–1855. doi:10.1016/j.ejca.2015.06.003
9. Enwere EK, Kornaga EN, Dean M, et al. Expression of PD-L1 and presence of CD8-positive T cells in pre-treatment specimens of locally advanced cervical cancer. *Mod Pathol*. 2017;30:577–586. doi:10.1038/modpathol.2016.221
10. Meng Y, Liang H, Hu J, et al. PD-L1 Expression correlates with tumor infiltrating lymphocytes and response to neoadjuvant chemotherapy in cervical cancer. *J Cancer*. 2018;9:2938–2945. doi:10.7150/jca.22532
11. Zhu X, Lang J. Soluble PD-1 and PD-L1: predictive and prognostic significance in cancer. *Oncotarget*. 2017;8:97671–97682. doi:10.18632/oncotarget.18311
12. Postow MA, Chesney J, Pavlick AC, et al. Nivolumab and ipilimumab versus ipilimumab in untreated melanoma. *N Engl J Med*. 2015;372:2006–2017. doi:10.1056/NEJMoa1414428
13. Robert C, G V L, Brady B, et al. Nivolumab in previously untreated melanoma without BRAF mutation. *New Eng J Med*. 2015;372:320–330. doi:10.1056/NEJMoa1412082
14. Omar HA, El-serafi AT, Hersi F, et al. Immunomodulatory MicroRNAs in cancer: targeting immune checkpoints and the tumor microenvironment. *FEBS J*. 2019;286:3540–3557. doi:10.1111/febs.15000
15. Chen AH, Qin YE, Tang WF, et al. MiR-34a and miR-206 act as novel prognostic and therapy biomarkers in cervical cancer. *Cancer Cell Int*. 2017;17:63. doi:10.1186/s12935-017-0431-9
16. Cortez MA, Ivan C, Valdecanas D, et al. PDL1 Regulation by p53 via miR-34. *J Natl Cancer Inst*. 2016;108:djv303. doi:10.1093/jnci/djv303
17. Huang P, You X, Pan M, et al. A novel therapeutic strategy using ultrasound mediated microbubbles destruction to treat colon cancer in a mouse model. *Cancer Lett*. 2013;335:183–190. doi:10.1016/j.canlet.2013.02.011
18. Chen F, Li Y, Feng Y, et al. Evaluation of antimetastatic effect of lncRNA-ATB siRNA delivered using ultrasound-targeted microbubble destruction. *DNA Cell Biol*. 2016;35:393–397. doi:10.1089/dna.2016.3254
19. Piscaglia F, Bolondi L. The safety of sonovue in abdominal applications: retrospective analysis of 23188 investigations. *Ultrasound Med Biol*. 2016;32:1369–1375. doi:10.1016/j.ultrasmedbio.2006.05.031
20. Porter TR, Iversen PL, Li S, et al. Interaction of diagnostic ultrasound with synthetic oligonucleotide-labeled perfluorocarbon exposed sonicated dextrose albumin microbubbles. *Ultrasound Med*. 1996;15:577–584. doi:10.7863/jum.1996.15.8.577
21. Zhou Q, Deng Q, Hu B, et al. Ultrasound combined with targeted cationic microbubble-mediated angiogenesis gene transfection improves ischemic heart function. *Exp Ther Med*. 2017;13:2293–2303. doi:10.3892/etm.2017.4270
22. Kopechek JA, Carson AR, Mctiernan CF, et al. Ultrasound targeted microbubble destruction-mediated delivery of a transcription factor decoy inhibits STAT3 signaling and tumor growth. *Theranostics*. 2015;5:1378–1387. doi:10.7150/thno.12822
23. Logana K, Fogliettaa F, Nesbitta H, et al. chemo-sonodynamic therapy treatment of breast tumours using ultrasound responsive microbubbles loaded with paclitaxel, doxorubicin and Rose Bengal. *Eur J Pharm*. 2019;139:224–231.
24. Song KH, Trudeau T, Kar A, et al. Ultrasound-mediated delivery of siESE complexed with microbubbles attenuates HER2± cell line proliferation and tumor growth in rodent models of breast cancer. *Nanotheranostics*. 2019;3:212–222. doi:10.7150/ntno.31827
25. Zhang L, Sun ZX, Ren PP, et al. Localized delivery of shRNA against PHD2 protects the heart from acute myocardial infarction through ultrasound-Targeted cationic microbubble destruction. *Theranostics*. 2017;7:51–66. doi:10.7150/thno.16074
26. Yang H, Cai W, Xu L, et al. Nanobubble-Affibody: novel ultrasound contrast agents for targeted molecular ultrasound imaging of tumor. *Biomaterials*. 2015;37:279–288. doi:10.1016/j.biomaterials.2014.10.013
27. Wang P, Yin T, Li J, et al. Ultrasound-responsive microbubbles for sonography-guided siRNA delivery. *Nanomedicine*. 2015;S1549963415006061.
28. Couto M, Cates C. Laboratory guidelines for animal care. *Methods Mol Biol*. 2019;1920:407–430.
29. Josefsson L, Goodall D, Emmer A. Implementation of a ultraviolet area imaging detector for analysis of polyvinyl alcohol microbubbles by capillary electrophoresis. *J Chromatogr A*. 2020. doi:10.1016/j.chroma.2020.460899
30. Brahmer JR, Drake CG, Wollner I. Phase I study of single-agent anti-programmed death-1 (MDX-1106) in refractory solid tumors: safety, clinical activity, pharmacodynamics, and immunologic correlates. *J Clin Oncol*. 2010;28:3167–3175. doi:10.1200/JCO.2009.26.7609
31. He J, Hu Y, Hu M, Li B. Development of PD-1/PD-L1 pathway in tumor immune microenvironment and treatment for non-small cell lung cancer. *Sci Rep*. 2015;13110. doi:10.1038/srep13110
32. Huang R, Rofstad EK. Cancer stem cells (CSCs), cervical CSCs and targeted therapies. *Oncotarget*. 2016;8:35351–35367.
33. Song H, Zhu J, Lu DH. Molecular-targeted first-line therapy for advanced gastric cancer. *Cochrane Database of Syst Rev*. 2016;7:CD011461.
34. Fan CH, Chang EL, Ting CY, et al. Folate-conjugated gene-carrying microbubbles with focused μltrasound for concurrent blood-brain barrier opening and local gene delivery. *Biomaterials*. 2016;106:46–57. doi:10.1016/j.biomaterials.2016.08.017
35. Yu J, Zhao Y, Liu C, et al. Synergistic anti-tumor effect of paclitaxel and miR-34a combined with ultrasound microbubbles on cervical cancer in vivo and in vitro. *Clin Transl Oncol*. 2019;15. doi:10.1007/s12094-019-02131-w

36. Franzen A, Vogt TJ, Muller T, et al. (CD274) and PD-L2 (PDCD1LG2) promoter methylation is associated with HPV infection and transcriptional repression in head and neck squamous cell carcinomas. *Oncotarget*. 2018;9:641–650. doi:10.18632/oncotarget.23080
37. Bommer GT, Gerin I, Feng Y, et al. p53-mediated activation of miRNA34 candidate tumor-suppressor genes. *Curr Biol*. 2007;17:1298–1307. doi:10.1016/j.cub.2007.06.068
38. Navarro F, Lieberman J. miR-34 and p53: new insights into a complex functional relationship. *PLoS One*. 2015;10:e0132767. doi:10.1371/journal.pone.0132767
39. Shetty SK, Tiwari N, Marudamuthu AS, et al. p53 and miR-34a feedback promotes lung epithelial injury and pulmonary fibrosis. *Am J Pathol*. 2017;187:1016–1034. doi:10.1016/j.ajpath.2016.12.020
40. Banta KL, Wang X, Das P, Winoto A. B cell lymphoma 2 (Bcl-2) residues essential for Bcl-2's apoptosis-inducing interaction with Nur77/Nor-1 orphan steroid receptors. *J Biol Chem*. 2018;293:4724–4734. doi:10.1074/jbc.RA117.001101
41. Liao LX, Zhao MB, Dong X, et al. TDB protects vascular endothelial cells against oxygen-glucose deprivation/reperfusion-induced injury by targeting miR-34a to increase Bcl-2 expression. *Sci Rep*. 2016;6:37959. doi:10.1038/srep37959
42. Li QL, Zhang HY, Qin YJ, et al. MicroRNA-34a promoting apoptosis of human lens epithelial cells through down-regulation of B-cell lymphoma-2 and silent information regulator. *Int J Ophthalmol*. 2016;9:1555–1560. doi:10.18240/ijo.2016.11.04
43. Wang Y, Wang L. miR-34a attenuates glioma cells progression and chemoresistance via targeting PD-L1. *Biotechnol Lett*. 2017;39:1485–1492. doi:10.1007/s10529-017-2397-z
44. Anastasiadou E, Stroopinsky D, Alimperti S, et al. Epstein−Barr virus-encoded EBNA2 alters immune checkpoint PD-L1 expression by downregulating miR-34a in B-cell lymphomas. *Leukemia*. 2019;33:132–147. doi:10.1038/s41375-018-0178-x